

The sign of active galactic nucleus quenching in a merger remnant with radio jets

Kohei ICHIKAWA^{1,*}, Junko UEDA¹, Megumi SHIDATSU², Taiki KAWAMURO³,
and Kenta MATSUOKA³

¹National Astronomical Observatory of Japan, 2-21-1 Osawa, Mitaka, Tokyo 181-8588, Japan

²MAXI team, RIKEN, 2-1 Hirosawa, Wako, Saitama 351-0198, Japan

³Department of Astronomy, Kyoto University, Kitashirakawa-Oiwake-cho, Sakyo-ku, Kyoto 606-8502, Japan

*E-mail: kohei.ichikawa@nao.ac.jp

Received ; Accepted

Abstract

We investigate optical, infrared, and radio active galactic nucleus (AGN) signs in the merger remnant Arp 187, which hosts luminous jets launched in the order of 10^5 yr ago but whose present-day AGN activity is still unknown. We find AGN signs from the optical BPT diagram and infrared [OIV]25.89 μm line, originating from the narrow line regions of AGN. On the other hand, *Spitzer*/IRS show the host galaxy dominated spectra, suggesting that the thermal emission from the AGN torus is considerably small or already diminished. Combining the black hole mass, the upper limit of radio luminosity of the core, and the fundamental plane of the black hole enable us to estimate X-ray luminosity, which gives $< 10^{40}$ erg s $^{-1}$. Those results suggest that the AGN activity of Arp 187 has already been quenched, but the narrow line region is still alive owing to the time delay of emission from the past AGN activity.

Key words: galaxies: active — galaxies: nuclei — infrared: galaxies

1 Introduction

A link between active galactic nuclei (AGN) and major galaxy mergers has been seen in luminous infrared galaxies (e.g., Sanders et al. 1988). Radial streaming motions during a merging event can efficiently feed gas to the central black hole (BH), and trigger AGN in late-stage mergers (e.g., Hopkins et al. 2006; Narayanan et al. 2008). The final stages of mergers are accompanied by a blow-out phase, expelling gas and dust into the intergalactic medium and quenching the star formation (e.g., Hopkins et al. 2008). Recent numerical simulations that include merger-driven fueling and “AGN feedback” reproduce several observed properties of the galaxy populations, such as the BH mass–bulge mass correlation or the rapid build-up of massive spheroids (e.g., Springel et al. 2005; Di Matteo et al. 2005). Therefore, AGN feedback has gradually been recognized as an important process in the evolution of galaxies.

Arp 187 is a merger remnant at the distance of $z = 0.04$ (and

the equivalent luminosity distance of $d_L = 171$ Mpc). Using ALMA Cycle 0 observations, Ueda et al. (2014) find two 3 mm continuum components located at both sides of the nucleus of Arp 187, spanning 4 kpc. These components are identified as small scale radio jets from high-resolution VLA archival images at 4.9 GHz and 8.5 GHz, which clearly show the morphology of the radio lobes. Assuming the jet angle to the line of sight of 90° and a typical expansion speed of radio lobes (0.1c; Murgia et al. 1999; Giroletti & Polatidis 2009), the kinematic age of the radio-jets is estimated to be 6×10^4 yr, which is quite young. Although the similar candidates have been found recently in the relatively distant universe at $z > 0.1$ (e.g., Komossa et al. 2006), as of our knowledge there are no candidates in the local universe with $z < 0.1$ due to their rare populations. Considering the properties above, Arp 187 is a good nearby candidate of AGN feedback study where AGN feedback has just started but not completed the star formation quenching (e.g., Matsushita

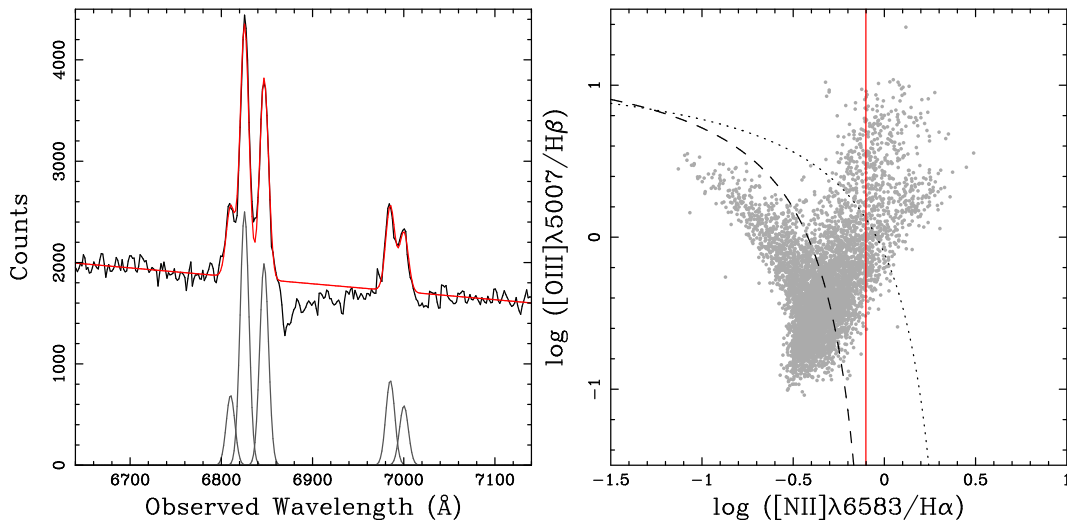


Fig. 1. (Left) The optical spectrum of Arp 187 around the $H\alpha$ line. The black/red solid line represents the obtained/fitted spectrum, respectively. Each gray lines represent the fitted line component, respectively. (Right) The location of Arp 187 (red solid line) in the BPT diagram. The dotted/dashed line represents the relation of Kauffmann et al. (2003)/Kewley et al. (2006), respectively. Gray dots represent the data points of SDSS DR7 galaxies (Abazajian et al. 2009).

et al. 2015, for the molecular gas and the jet interaction study).

While Arp 187 has radio-jets, it is still not clear whether its AGN activity is still on-going due to the absence of previous studies. The most secure way to identify AGN is a hard X-ray observation, because there is no strong bias against absorption up to $\log N_H \sim 24.5$ based on theoretical (e.g., Brightman & Nandra 2011) and observational studies (e.g., Ichikawa et al. 2012). However, the 70-month integration of *Swift*/BAT 14–195 keV all-sky survey (Baumgartner et al. 2013) did not detect Arp 187, constraining the luminosity of $\log L_{14-195\text{keV}} \leq 43.7$. This suggests that AGN activity in Arp 187 might be already weakened and/or obscured. Infrared (IR) observations give us another secure way to find AGN since the AGN dust torus emission is dominated in mid-IR (Imanishi et al. 2011; Ichikawa et al. 2012, 2014, 2015). Utilizing the *Spitzer* mid-IR imaging data, Ohya et al. (2015) found AGN signs in the southern nucleus of NGC 3256 hosting molecule outflows (Sakamoto et al. 2014). Alonso-Herrero et al. (2012) observed *Spitzer*/IRS 5–38 μm spectra of LIRGs and decomposed the spectra into starburst (SB) and AGN components using a SB galaxy template and clumpy torus models (Nenkova et al. 2008) supported by observations (Gandhi et al. 2009; Ichikawa et al. 2012; Shirahata et al. 2013; Markowitz et al. 2014; Asmus et al. 2015). In this letter, we report the investigation of AGN activity embedded in Arp 187 through the optical, IR, and radio-band studies. Throughout the paper, we adopt $H_0 = 70.0 \text{ km s}^{-1} \text{ Mpc}^{-1}$, $\Omega_M = 0.3$, $\Omega_\Lambda = 0.7$.

2 Optical Spectra

The optical spectra enable us to disentangle type-2 AGN and starburst galaxy using the optical line ratios. Considering AGN

have harder spectra than the galaxies, the line ratio with a different ionization potential gives a good separation between the narrow line region (NLR) gas ionized by AGN and HII region (called BPT diagram; Baldwin et al. 1981; Veilleux & Osterbrock 1987). We examined an archival optical spectrum obtained by the 6dF galaxy survey (Jones et al. 2009). It is noted that the spectra of 6dF survey are not properly flux calibrated, but the flux ratio of adjacent lines is still useful. The spectrum covers a range from 3900 Å to 7500 Å with the fiber aperture of 6.7 arcsec (equivalent to $\sim 5.6 \text{ kpc}$ at $z = 0.04$). Although there is a clear detection of crucial line sets for the BPT diagram including $H\beta$, $[\text{OIII}]\lambda 5007$, $H\alpha$, and $[\text{NII}]\lambda 6583$, one should use caution to obtain $H\beta$ line flux as the additional spectral decomposition is necessary to estimate how much the $H\beta$ absorption line from the host galaxy affects the observed $H\beta$ emission line. Therefore, we used $[\text{N II}]\lambda 6584/H\alpha$ only because the concern above should be negligible for these two lines (e.g., Lee et al. 2011). The left panel of figure 1 shows the spectrum of Arp 187 around the $H\alpha$ line. The derived flux ratio of $[\text{N II}]\lambda 6584/H\alpha$ is 0.79. The right panel of figure 1 shows where Arp 187 locates in the BPT diagram. Above/below the dotted/dashed line is the locus of AGN/starburst galaxy, respectively. The location between the two lines between Kauffmann et al. (2003) (dotted) and Kewley et al. (2006) (dashed) is called composite area where the galaxy has an AGN, but the strong contribution from the host galaxy. This shows that Arp 187 belongs to a composite galaxy, LINER, or AGN locus.

One caveat for this result is that the stellar absorption at the $H\alpha$ line could affect the position of BPT diagram. To check this effect, we measured $H\alpha$ absorption strength from the spectrum template of elliptical galaxy in Kinney et al. (1996), resulting the estimated equivalent width is small with $\sim 1 \text{ Å}$. Considering

H α equivalent width of Arp 187 is ~ 20 , the effect is only $\sim 5\%$, shifting the ratio of [NII]/H α from 0.79 to 0.74. This does not change our main result. Another caveat is that the observed [N II] $\lambda 6584$ /H α could be shifted by a radio-jet shock excitation. Allen et al. (2008) showed that fast shock can mimic the position of the source into the AGN locus in the BPT diagram if the galaxy emission is fully dominated by shocks. However, in reality, shocks rarely dominate a galaxy's global emission (e.g., Kewley et al. 2013). Using the large sample of radio-loud and radio-quiet AGN in the SDSS survey, Kauffmann et al. (2008) showed that both AGN locate remarkably similar positions in the BPT diagram, suggesting that the radio-shock contribution could be negligible for most of the radio-loud sources in the local universe. Further checks on the radio-jet contribution will be explored after obtaining the flux calibrated high spatial optical spectra or Integral Field Unit (IFU).

3 IR Spectra

3.1 *Spitzer*/IRS spectra

We obtained *Spitzer*/IRS low-resolution 5.0–38.0 μm spectra from Cornell Atlas of *Spitzer*/IRS Sources (CASSIS; Lebouteiller et al. 2011). As CASSIS identified Arp 187 as an extended source with a spatial extent of 4.5 arcsec, it used the extraction aperture width which scales with the spatial extent to account for all of the source's flux.

The obtained IRS spectra include the [OIV]25.89 μm line with an ionization potential of $E_p = 54.9$ eV (Rigby et al. 2009), which is one of the indicators of AGN and small contamination from the starburst ($\sim 5\%$ of the line flux in AGN on average; Pereira-Santaella et al. 2010). The spectra of Arp 187 shows a marginal detection of the [OIV]25.89 μm line at $S/N \sim 3$, suggesting a weak AGN NLR activity. The line luminosity of [OIV]25.89 μm was obtained with $L_{[\text{OIV}]} = 6.7 \times 10^{40}$ erg s $^{-1}$. Using the large sample of nearby AGN that have both of X-ray and *Spitzer*/IRS spectra, Liu et al. (2014) showed the clear luminosity relations between $L_{[\text{OIV}]}$ and $L_{2-10\text{keV}}$, $L_{14-195\text{keV}}$. Using the relation of Liu et al. (2014), estimated X-ray luminosities are $L_{2-10\text{keV}} = 2.5 \times 10^{42}$ erg s $^{-1}$ and $L_{14-195\text{keV}} = 8.9 \times 10^{42}$ erg s $^{-1}$. LaMassa et al. (2010) also reported the relationship between $L_{[\text{OIV}]}$ and AGN 13.5 μm MIR continuum luminosity $L_{\text{MIR}}^{(\text{AGN})}$, $L_{14-195\text{keV}}$ suggesting that the expected $L_{\text{MIR}}^{(\text{AGN})} = 1.9 \times 10^{43}$ erg s $^{-1}$ and $L_{14-195\text{keV}} = 1.4 \times 10^{43}$ erg s $^{-1}$, respectively. Note that the intrinsic scatter of each luminosity-luminosity relations is large with ~ 0.3 – 0.5 dex.

3.2 Thermal emission from AGN torus

We decompose the IRS spectra into a combination of stellar direct, host galaxy, and AGN. We use the IDL routine of Hernán-Caballero et al. (2015) called DeblendIRS. It prepares

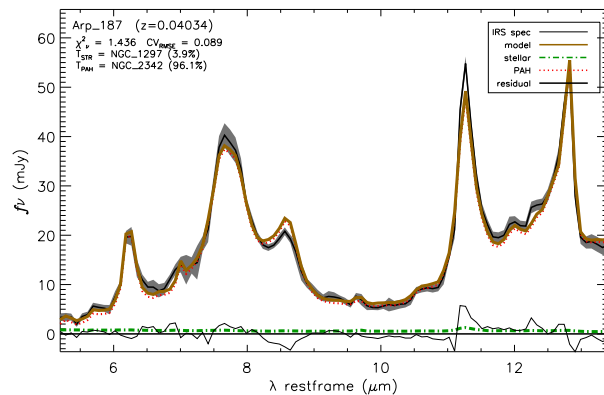


Fig. 2. The *Spitzer*/IRS spectra of Arp 187. The brown line represents the model spectra of STR+PAH component obtained from deblendIRS. The green dashed-dot/red dotted line represents the STR and PAH component, respectively.

a linear combination of three spectral templates of AGN, the stars (“STR”), and the interstellar medium of the host galaxy (“PAH”), all of which are selected from a large library of IRS spectra from the sources with “pure-AGN”, “pure-stellar”, and “pure-interstellar” spectra. A further description of the decomposition method is given in Section 2 of Hernán-Caballero et al. (2015). We apply this spectral decomposition routine to the obtained IRS spectra. We only use the IRS short band (5.0–14.0 μm) to follow the same manner as Hernán-Caballero et al. (2015). They noted that it is difficult to distinguish between the continuum emission of the AGN and the host at the longer wavelength with $\lambda > 14$ μm . In addition, the fraction of the total continuum from the AGN decrease drastically at longer wavelength with the combined effects of a steeply rising emission from dust heated by star formation.

In order to check whether an AGN component contribute to the IR spectra, we first fit the IRS only with STR+PAH component. The best fitting result is achieved with the STR contribution of 3.9% and PAH contribution of 96.1%. The PAH is the dominant component in the spectra as shown in Figure 2. The resultant reduced χ^2 value is $\chi^2/\text{dof} = 142.3/99 = 1.437$. Then we fit the spectra again with STR+PAH+AGN component. The best fit is achieved with the STR contribution of 3.0%, PAH contribution of 95.5%, and AGN contribution of 1.6% with the reduced χ^2 value of $\chi^2/\text{dof} = 139.8/98 = 1.427$. The improvement of the fit based on the F-test shows that the probability is $P = 0.196$, which is larger than 0.05, suggesting that the addition of AGN component does not give significant improvement to explain the spectra. Therefore we conclude that the thermal emission from AGN is already weak or diminished in Arp 187.

One caveat is the possibility that the thermal emission from AGN is hidden within the scatter of the IRS spectra. The averaged S/N at each bin of the spectra with $\sim S/N = 10$ enables us to give an upper limit of AGN torus thermal emission. The upper limit of AGN 12 μm luminosity is $L_{12\mu\text{m}} =$

$1.5 \times 10^{42} \text{ erg s}^{-1}$. Using the $L_{2-10\text{keV}}-L_{12\mu\text{m}}$ luminosity relations of nearby Seyfert galaxies obtained by Gandhi et al. (2009), $L_{2-10\text{keV}} = 2.8 \times 10^{42} \text{ erg s}^{-1}$. The estimated BAT X-ray luminosity is $L_{14-195\text{keV}} = 5.9 \times 10^{42} \text{ erg s}^{-1}$ using the ratio of 2.1 under the assumption of photon index of $\Gamma = 1.9$ (Nemmen et al. 2011). This is consistent with the non-detection at *Swift*/BAT survey. Comparing the luminosities with those expected from [OIV] 25.89 μm lines are insightful because the AGN thermal emission originates from the central $< 10 \text{ pc}$, while [OIV] 25.89 μm line emission would arise from the NLR with $\sim 1 \text{ kpc}$ scale. The upper limit of $L_{12\mu\text{m}}$ is one order of magnitude smaller than the expected $L_{\text{MIR}}^{(\text{AGN})}$ from [OIV] 25.89 μm line. The upper limit of X-ray luminosities are comparable or slightly smaller than the expected value from [OIV] 25.89 μm lines.

On the intrinsic nuclear AGN activity, final check should be done by direct high sensitive X-ray observations. *NuSTAR* (Harrison et al. 2013) and/or *ASTRO-H* (Takahashi et al. 2014) give us the detailed information including the hard X-ray ($E > 10 \text{ keV}$) band (Brightman et al. 2015). The spectra can be obtained in 3–70 keV band with 40 ksec exposure up to $N_{\text{H}} < 10^{24} \text{ cm}^{-2}$ under the assumption of photon index of $\Gamma = 1.9$ (Nemmen et al. 2011). Even in the Compton-thick case with $N_{\text{H}} \leq 3 \times 10^{24} \text{ cm}^{-2}$, the detection can be achievable with the $\text{S/N} = 4.5$ around 10–20 keV band. Therefore, the future X-ray observations are effective and highly encouraged to confirm whether or not the AGN activity exists in Arp 187.

Another caveat is the contamination from the jet synchrotron emission to the IRS spectra. We check the contribution of jet-emission in the IRS band by extrapolating the power-law obtained from the radio bands between 80 MHz and 10 GHz from NASA/IPAC Extragalactic Database (NED). The contribution of the extrapolated IR emission is three orders of magnitude lower than the observed spectra by *Spitzer*/IRS, therefore we conclude the jet-contamination in the IRS band for Arp 187 is negligible.

4 Constraint of AGN activity through the BH fundamental plane

The fundamental plane of BH activity gives a relation among X-ray luminosity, core radio luminosity and the BH mass (Merloni et al. 2003; Heinz & Sunyaev 2003; Yuan & Narayan 2014). Based on the nucleus *K* band photometry in Rothberg & Joseph (2004), Arp 187 has a stellar mass of $M_{\text{stellar}} = 1.3 \times 10^{11} M_{\odot}$ with Sérsic index of $n = 4.1$, suggesting that Arp 187 has a bulge dominated galaxy. Therefore, $M_{\text{bulge}} \simeq M_{\text{stellar}}$. Using the $M_{\text{BH}}-M_{\text{bulge}}$ scaling relation of Kormendy & Ho (2013), the estimated mass $M_{\text{BH}} = 6.7 \times 10^8 M_{\odot}$ is given. The central core ($\lesssim 0.42 \text{ arcsec}$, which is equivalent to $\lesssim 300 \text{ pc}$) of Arp 187 is not detected in the VLA 4.9 GHz archival image,

and the 3σ upper limit of the radio flux is $210 \mu\text{Jy}$, corresponding to $L_{\text{R}} \leq 3.7 \times 10^{37} \text{ erg s}^{-1}$. Combining those two parameters and the equation of the updated fundamental plane of Gültekin et al. (2009) enables us to derive the upper limit of 2–10 keV luminosity with $L_{2-10\text{keV}} < 6.6 \times 10^{36} \text{ erg s}^{-1}$. Some studies suggest that a low-Eddington case might follow the different fundamental relation (Yuan & Cui 2005). The nucleus of Arp 187 could be in those cases. Applying the relation of Yuan & Cui (2005) gives a larger upper limit of $L_{2-10\text{keV}} < 4.0 \times 10^{39} \text{ erg s}^{-1}$. Either case is consistent with the result of very weak or absent of thermal emission of AGN discussed in Section 3.

5 Discussion and Summary

We discuss the results of our optical, IR, and radio studies. While Arp 187 hosts small jets with the age of $\sim 6 \times 10^4 \text{ yr}$, the non-detection of the radio-core and weak or diminished thermal emission from AGN torus in the IR band prefers the absence of an AGN activity in Arp 187, therefore we conclude that the galaxy's central engine has decreased the energy output by at least a few orders of magnitude within $6 \times 10^4 \text{ yr}$.

The results of optical BPT diagram and the marginal detection of [OIV] 25.89 μm indicate that the NLR of Arp 187 is still alive. Considering the size of NLR is larger for three to four order of magnitude (1–10 kpc) compared to the thermal emission region (called torus; $< 10 \text{ pc}$; Bartscher et al. 2013) of AGN, NLR activity traces the past activity at least 10^{4-5} yr ago considering the light travel time from the central engine to the NLR (same method was employed by the authors of Dadina et al. 2010; Keel et al. 2012). This is consistent with the sign of past activity in the radio-jet and its age is $6 \times 10^4 \text{ yr}$. Combining all the results, AGN in Arp 187 was active at least 10^{4-5} yr ago, but it is already quenched now and only the extended area leaves the signature of past AGN activity. The similar type of populations were reported previously. One is called changing-look AGN. LaMassa et al. (2015) reported the fading AGN that experienced over one order of magnitude optical/X-ray flux declining within 10 yr and drastic disappearance of broad $\text{H}\beta$ component. This change might be caused by the declining of accretion rate (Elitzur et al. 2014). Another similar population is called “Hanny’s Voorwerp”, which has a faded central engine, but the larger scale NLR emission has been seen as the light echo of AGN (Lintott et al. 2009; Keel et al. 2012; Schawinski et al. 2015). These studies of Voorwerps estimate the quenching time scale to 10^{4-5} yrs via the geometry of their spatial extent.

One question arises how the sudden quenching of AGN occurs within 10^{4-5} yr . Schawinski et al. (2010) discussed the possibility of such short quenching time scale of AGN with an analogy of X-ray black hole binary study. State changes of GRS 1915+105 with a BH mass of $10 M_{\odot}$ occur with the time scale

of 1 hr. Extrapolating the BH mass-time variation relation above to Arp 187 with $M_{\text{BH}} = 6.7 \times 10^8 M_{\odot}$, the state change can occur with the time scale of $\sim 10^4$ yr, which is in accordance with the estimated time scale from NLR and radio-jet within an order of magnitude. This also may support that Arp 187 has experienced the state transition from a high state to a radiatively inefficient state where the energy is released mainly as kinetic energy (Ichimaru 1977; Narayan & Yi 1994). The presence of a radio-jet also favors the hypothesis above if the launch of the jet is associated with the state change. Arp 187 is a good nearby candidate for future observations of both central engine with *Nustar*, *ASTRO-H* and the host galaxy with ALMA to answer how the AGN is going to die and affects the environment of the host galaxy.

Acknowledgments

We are grateful for useful comments from the anonymous referee. We thank Yoshiki Matsuoka, Tohru Nagao, Ryou Ohsawa, Kouji Ohta, Chris Packham, and Yoshihiro Ueda for valuable comments and discussions. This research has made use of the NASA/IPAC Extragalactic Database (NED) which is operated by the Jet Propulsion Laboratory, California Institute of Technology, under contract with the National Aeronautics and Space Administration. This work was partly supported by the Grant-in-Aid for Scientific Research 40756293 (K.I.).

References

- Abazajian, K. N., Adelman-McCarthy, J. K., Agüeros, M. A., et al. 2009, *ApJS*, 182, 543
- Allen, M. G., Groves, B. A., Dopita, M. A., Sutherland, R. S., & Kewley, L. J. 2008, *ApJS*, 178, 20
- Alonso-Herrero, A., Sánchez-Portal, M., Ramos Almeida, C., et al. 2012, *MNRAS*, 425, 311
- Asmus, D., Gandhi, P., Hoenig, S. F., Smette, A., & Duschl, W. J. 2015, *arXiv:1508.05065*
- Baldwin, J. A., Phillips, M. M., & Terlevich, R. 1981, *PASP*, 93, 5
- Baum, S. A., Zirbel, E. L., & O’Dea, C. P. 1995, *ApJ*, 451, 88
- Baumgartner, W. H., Tueller, J., Markwardt, C. B., et al. 2013, *ApJS*, 207, 19
- Brightman, M., & Nandra, K. 2011, *MNRAS*, 413, 1206
- Brightman, M., Baloković, M., Stern, D., et al. 2015, *ApJ*, 805, 41
- Burtscher, L., Meisenheimer, K., Tristram, K. R. W., et al. 2013, *A&A*, 558, A149
- Dadina, M., Guainazzi, M., Cappi, M., et al. 2010, *A&A*, 516, A9
- Di Matteo, T., Springel, V., & Hernquist, L. 2005, *Nature*, 433, 604
- Elitzur, M., Ho, L. C., & Trump, J. R. 2014, *MNRAS*, 438, 3340
- Gandhi, P., Horst, H., Smette, A., et al. 2009, *A&A*, 502, 457
- Giroletti, M., & Polatidis, A. 2009, *Astronomische Nachrichten*, 330, 193
- Gültekin, K., Cackett, E. M., Miller, J. M., et al. 2009, *ApJ*, 706, 404
- Harrison, F. A., Craig, W. W., Christensen, F. E., et al. 2013, *ApJ*, 770, 103
- Heinz, S., & Sunyaev, R. A. 2003, *MNRAS*, 343, L59
- Hernán-Caballero, A., Alonso-Herrero, A., Hatziminaoglou, E., et al. 2015, *ApJ*, 803, 109
- Hopkins, P. F., Cox, T. J., Kereš, D., & Hernquist, L. 2008, *ApJS*, 175, 390
- Hopkins, P. F., Hernquist, L., Cox, T. J., et al. 2006, *ApJS*, 163, 1
- Ichikawa, K., Ueda, Y., Terashima, Y., et al. 2012, *ApJ*, 754, 45
- Ichikawa, K., Imanishi, M., Ueda, Y., et al. 2014, *ApJ*, 794, 139
- Ichikawa, K., Packham, C., Ramos Almeida, C., et al. 2015, *ApJ*, 803, 57
- Ichimaru, S. 1977, *ApJ*, 214, 840
- Ikeda, S., Awaki, H., & Terashima, Y. 2009, *ApJ*, 692, 608
- Imanishi, M., Imase, K., Oi, N., & Ichikawa, K. 2011, *AJ*, 141, 156
- Jones, D. H., Read, M. A., Saunders, W., et al. 2009, *MNRAS*, 399, 683
- Kauffmann, G., Heckman, T. M., Tremonti, C., et al. 2003, *MNRAS*, 346, 1055
- Kauffmann, G., Heckman, T. M., & Best, P. N. 2008, *MNRAS*, 384, 953
- Keel, W. C., Chojnowski, S. D., Bennert, V. N., et al. 2012, *MNRAS*, 420, 878
- Kewley, L. J., Groves, B., Kauffmann, G., & Heckman, T. 2006, *MNRAS*, 372, 961
- Kewley, L. J., Dopita, M. A., Leitherer, C., et al. 2013, *ApJ*, 774, 100
- Kinney, A. L., Calzetti, D., Bohlin, R. C., et al. 1996, *ApJ*, 467, 38
- Komossa, S., Voges, W., Xu, D., et al. 2006, *AJ*, 132, 531
- Kormendy, J., & Ho, L. C. 2013, *ARA&A*, 51, 511
- LaMassa, S. M., Heckman, T. M., Ptak, A., et al. 2010, *ApJ*, 720, 786
- LaMassa, S. M., Cales, S., Moran, E. C., et al. 2015, *ApJ*, 800, 144
- Lebouteiller, V., Barry, D. J., Spoon, H. W. W., et al. 2011, *ApJS*, 196, 8
- Lee, J. C., Hwang, H. S., Lee, M. G., Kim, M., & Kim, S. C. 2011, *MNRAS*, 414, 702
- Lintott, C. J., Schawinski, K., Keel, W., et al. 2009, *MNRAS*, 399, 129
- Liu, T., Wang, J.-X., Yang, H., Zhu, F.-F., & Zhou, Y.-Y. 2014, *ApJ*, 783, 106
- Markowitz, A. G., Krumpe, M., & Nikutta, R. 2014, *MNRAS*, 439, 1403
- Matsushita, S., Trung, D.-V., Boone, F., et al. 2015, *ApJ*, 799, 26
- Merloni, A., Heinz, S., & di Matteo, T. 2003, *MNRAS*, 345, 1057
- Murgia, M., Fanti, C., Fanti, R., et al. 1999, *A&A*, 345, 769
- Narayanan, D., Cox, T. J., Kelly, B., et al. 2008, *ApJS*, 176, 331
- Narayan, R., & Yi, I. 1994, *ApJL*, 428, L13
- Nemmen, R., Storchi-Bergmann, T., & Eracleous, M. 2011, *arXiv:1112.4640*
- Neškova, M., Sirocky, M. M., Ivezić, Ž., & Elitzur, M. 2008, *ApJ*, 685, 147
- Ohya, Y., Terashima, Y., & Sakamoto, K. 2015, *arXiv:1503.08555*
- Pereira-Santaella, M., Diamond-Stanic, A. M., Alonso-Herrero, A., & Rieke, G. H. 2010, *ApJ*, 725, 2270
- Rigby, J. R., Diamond-Stanic, A. M., & Aniano, G. 2009, *ApJ*, 700, 1878
- Rothberg, B., & Joseph, R. D. 2004, *AJ*, 128, 2098
- Sakamoto, K., Aalto, S., Combes, F., Evans, A., & Peck, A. 2014, *ApJ*, 797, 90
- Sanders, D. B., Soifer, B. T., Elias, J. H., Neugebauer, G., & Matthews, K. 1988, *ApJL*, 328, L35
- Schawinski, K., Evans, D. A., Virani, S., et al. 2010, *ApJL*, 724, L30
- Schawinski, K., Koss, M., Berney, S., & Sartori, L. F. 2015, *MNRAS*, 451, 2517
- Scott, N., Graham, A. W., & Schombert, J. 2013, *ApJ*, 768, 76
- Shirahata, M., Nakagawa, T., Usuda, T., et al. 2013, *PASJ*, 65, 5
- Springel, V., White, S. D. M., Jenkins, A., et al. 2005, *Nature*, 435, 629
- Takahashi, T., Mitsuda, K., Kelley, R., et al. 2014, *Proc. SPIE*, 9144, 914425
- Ueda, J., Iono, D., Yun, M. S., et al. 2014, *ApJS*, 214, 1
- Veilleux, S., & Osterbrock, D. E. 1987, *ApJS*, 63, 295
- Yuan, F., & Cui, W. 2005, *ApJ*, 629, 408
- Yuan, F., & Narayan, R. 2014, *ARA&A*, 52, 529